

11/30/2023

## Part I

# Numerical-Analytical Analysis on SCCP

In this study an appropriate expression to estimate the output power of solar chimney power plant systems (SCPPS) was considered. Recently several mathematical models of SCPPS were derived, studied for a variety of boundary conditions, and compared against CFD calculations. An important concern for modeling SCPPS is the accuracy of the derived pressure drop and output power equation. To elucidate the matter, axisymmetric CFD analysis was performed to model the solar chimney power plant and calculate the output power for different available solar radiation.

Both analytical and numerical results were compared against the available experimental data from the historical Manzanares power plant. We also evaluated the fidelity of the assumptions underlying the derivation and present the output power characteristics of Manzanares prototype under a range of solar irradiation, mass flow rate and collector efficiency. This research provides an approach to estimate the output power with respect to available radiation to the collector .

Collector Chimney Pressure drop Modeling and simulation Analytical solution  
Computational fluid dynamics

## **Nomenclature**

### *Variables*

$A$	cross-sectional area, $m^2$
$A_r$	cross-sectional area of the collector ground, $m^2$
$g$	acceleration due to gravity, $m/s^2$
$h$	height, $m$
$\dot{m}$	air mass flow rate, $kg/s$
$p$	pressure, $N/m^2$
$\dot{W}$	flow power, $W$
$q$	heat transfer per unit mass, $J/kg$
$q''$	heat flux, $W/m^2$
$R$	air specific gas constant, $J/kg.K$
$T$	temperature, $K$

$\rho$  density,  $kg/m^3$   
 $u$  velocity,  $m/s$   
 $c_p$  specific heat capacity,  $J/kg.K$

*Subscripts*

$i$  inlet  
 $o$  outlet  
 $c$  collector  
 $t$  tower  
 $m$  mean  
 $\infty$  ambient air  
 $turb$  turbine  
 $atm$  atmospheric

*Abbreviations*

*CFD* computational Fluid Dynamics  
*EOS* equation of state  
*SCPPS* solar chimney power plant system  
*RHS* right hand side  
*M&S* modeling and simulation

## **1.1 Introduction**

Although the idea of the SCPPS can be traced to the early 20th century, practical investigations of solar power plant systems started in the late 1970s, around the time of conception and construction of the first prototype in Manzanares, Spain. This solar power plant operated between 1982 and 1989 and the generated electric power was used in the local electric network [1–3].

The basic SCPPS concept (Fig. 1.1) demonstrated in that facility is fairly straightforward. Sunshine heats the air beneath a transparent roofed collector structure surrounding the central base of a tall chimney. The hot air produces an updraft flow in the chimney. The energy of this updraft flow is harvested with a turbine in the chimney, producing electricity. Experiments with the prototype proved the concept to be viable, and provided data used by a variety of later researchers. A major motivation for subsequent studies lays in the need for reliable modeling of the operation of a large-scale power plant. The Manzanares prototype had a 200 m tall chimney and a 40,000 m<sup>2</sup> collector area. With respect to the distinguished rise of R&D budget on renewable energy [5], study and evaluation the different aspects of SCPPS seem beneficial and vital. Proposals for economically competitive SCPPS facilities usually feature chimneys on the scale of 1 km and collectors with multiple square kilometer areas.

Padki and Sherif [6] used the results from the Manzanares prototype to extrapolate the data to large scale models for SCPPS. In 1991, Yan et al. [7] developed

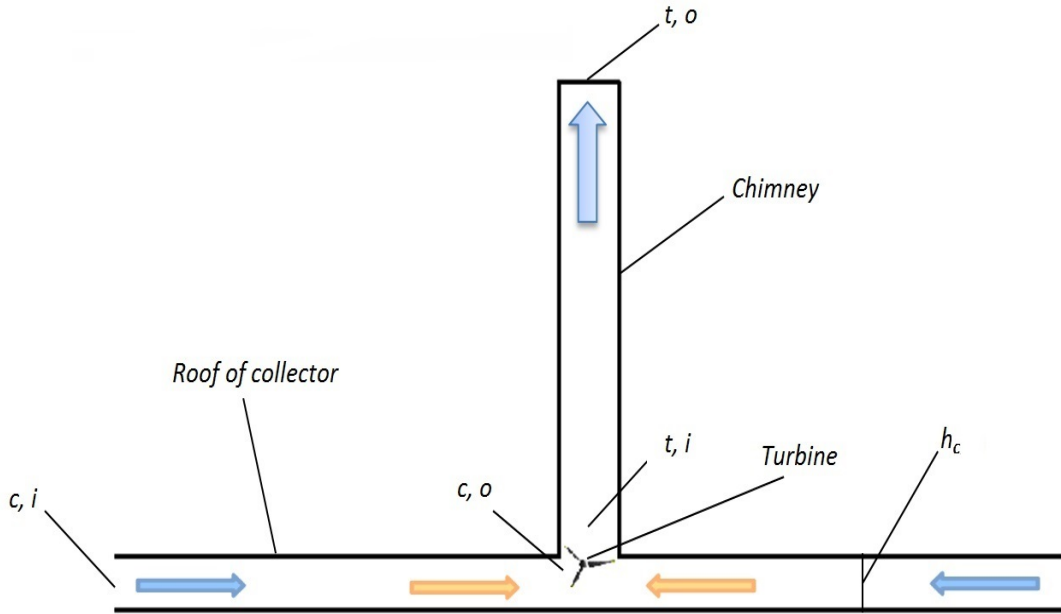


FIGURE 1.1: Schematic of SCPPS with the applied variables and subscripts in the present analysis

an SCPPS model using a practical correlation. They introduced equations including air velocity, air flow rate, output power, and thermofluid efficiency. Von Backström and Fluri conducted a numerical study to determine the optimum ratio of pressure drop of the turbine as a fraction of the available pressure difference required to achieve the maximum power [8]. They noted that this ratio might lead to overestimating the flow passage in the plant and also designing a turbine without a sufficient stall margin. In other recent works, the SCPPS concept involving an inflatable tower was examined, with all parts of the power plant modeled numerically [9–11].

To find the maximum power, different atmospheric pressure and temperature boundary conditions were applied for various tower heights and atmospheric lapse rates [12, 13]. Theoretical analysis to study the effect of pressure drop in the

SCPPS turbine was performed by Koonsrisuk et al. [14]. The optimal pressure drop ratio was found numerically and analytically by Xu et al., around 0.9 for the Manzanares prototype. This investigation can be applied as an initial estimation for various SCPPS turbines [15].

Earlier modeling efforts [9] showed a keen sensitivity of the predictions of SCPPS output to boundary conditions, in particular, pressure. Numerical simulations require careful validation and verification, and for that, analytical models are indispensable. A theoretical model was recently developed [16] to model the combined performance of the solar collector, chimney, and turbine. Here we will examine some of the assumptions and derivations in this model and present an alternative formulation for the energy equation. We will perform M&S of the Manzanares prototype and compare the computational results against the available experimental values and our analytical analysis data. This comparative study is carried out for different solar radiation based on available experimental data.

## **1.2 Analytical Study**

### **1.2.1 Collector**

Solar Chimney Power Plants provide a reliable and conceptually straightforward way of energy generation from the solar irradiation[14, 17]. A solar collector is the main and only component of this power plant to accumulate the available solar energy to heat up air in a greenhouse. The air escapes the collector through a

tall chimney which connects the warm air flow of the collector with the cooler air above the ground. The temperature difference induces the natural convection, and turbine at the outlet of collector harvests the energy of the air flow. To model the collector, the simplified one dimensional mathematical analysis was performed to clarify the details. The analytical correlation will be applied later to compare the CFD results against it. To derive the equations, we start from the collector. It is assumed that the flow through the collector is one-dimensional, steady-state, and compressible. Let us disregard the friction and assume the total heat from the solar irradiation is absorbed within the air filling the collector. For this thermal-fluid analysis, the mass conservation satisfies:

$$\frac{dA}{A} + \frac{d\rho}{\rho} + \frac{du}{u} = 0 \quad (\text{Continuity}) \quad (1.1)$$

Here  $A$  is the cross-sectional area of the collector that air goes through –  $A = 2\pi r h_c$  and  $dA = 2\pi r dh_c$ .

Momentum equation is as follows:

$$dp + \rho u du = 0 \quad (\text{Momentum}) \quad (1.2)$$

Consider the energy balance equation and the equation of state as follows:

$$c_p dT - dq + u du = 0 \quad (\text{Energy}) \quad (1.3)$$

$$dp = d(\rho RT) \quad (\text{State}) \quad (1.4)$$

To find  $dp$  we can apply Eq. (1.2) and substitute  $du/u$  from the continuity equation, Eq. (1.1).

$$dp = \rho u^2 \left( \frac{d\rho}{\rho} + \frac{dA}{A} \right) \quad (1.5)$$

From the equation of state we can find  $d\rho/\rho$  and substitute in Eq. (1.5),

$$\frac{d\rho}{\rho} = \frac{dp}{p} - \frac{dT}{T} \quad (1.6)$$

$$dp = \rho u^2 \left( \frac{dp}{p} - \frac{dT}{T} + \frac{dA}{A} \right) \quad (1.7)$$

We can rewrite Eq. (1.7) as a function of  $T, A, u, p, \rho$  and  $\dot{m}$ , where  $\dot{m} = \rho Au$ . Also by substitution  $dT$  from the energy equation on the base of  $dq, c_p$  and  $u$ , we obtain

$$dp = \frac{\dot{m}^2}{\rho} \left( \frac{dA}{A^3} - \frac{dq - udu}{A^2 T c_p} + \frac{dp}{A^2 p} \right) \quad (1.8)$$

For consistency with previous analyses, let us rewrite  $dq$  on the basis of heat flux, available solar insolation to the air, per mass flow rate— $dq = q'' dA_r / \dot{m}$  where  $q$  has the units of  $J/kg$ . Here  $A_r = \pi r^2$ , therefore  $dA_r = 2\pi r dr$  [14, 18]. Note that

$A = 2\pi r h_c$ , where  $h_c$  is the collector height (roof height) that was assumed to be constant. By substituting  $A_r$ ,  $dq$  and  $A$  in the second term on the RHS, we obtain

$$dp = \frac{\dot{m}^2}{\rho} \left( \frac{dA}{A^3} - \frac{q''(2\pi r)dr}{\dot{m}(2\pi r h_c)^2 T c_p} + \frac{udu}{A^2 c_p T} + \frac{dp}{A^2 p} \right) \quad (1.9)$$

We can rewrite equation (1.9) and substitute  $udu$  of the third term on the RHS by applying momentum equation (1.2),  $udu = -dp/\rho$  and  $p = \rho RT$ .

$$dp = \frac{\dot{m}^2}{\rho} \left[ \frac{dA}{A^3} - \frac{q'' dr}{2\pi \dot{m} r h_c^2 c_p T} \right] \left[ 1 - \frac{u^2}{T} \left( \frac{1}{R} - \frac{1}{c_p} \right) \right]^{-1} \quad (1.10)$$

Equation (1.10) is the exact solutions for  $dp$  for the one-dimensional frictionless analysis of the collector. Since our fluid is air we can estimate  $c_p$  and rewrite Eq. (1.10).

$$dp \simeq \frac{\dot{m}^2}{\rho} \left( \frac{dA}{A^3} - \frac{q'' dr}{2\pi \dot{m} r h_c^2 c_p T} \right) \left( 1 - \frac{2.494u^2}{T} \right)^{-1} \quad (1.11)$$

$c_p$ ,  $q''$  and  $T$  are considered approximately constant as well. The last term on the RHS of (1.11) is close to unity within the range of velocities and temperatures under consideration. Therefore by integrating between the inlet and outlet of the collector without the last term of the RHS, pressure difference can be derived.

$$\int_{c,i}^{c,o} dp \simeq \int_{c,i}^{c,o} \left( \frac{\dot{m}^2 dA}{\rho A^3} - \frac{\dot{m} q'' dr}{2\pi r h_c^2 \rho c_p T} \right) \quad (1.12)$$

$$p_{c,o} - p_{c,i} \simeq \left[ \frac{\dot{m}^2}{2\rho_{m,c}} \left( \frac{1}{A_{c,i}^2} - \frac{1}{A_{c,o}^2} \right) + \frac{q'' \dot{m}}{2\pi h_c^2 c_p \rho_{m,c} T_{m,c}} \ln \frac{r_{c,i}}{r_{c,o}} \right] \quad (1.13)$$

Equation (1.13) represents the pressure difference along the collector due to change in the flow area (first term) and as a result of the solar radiation (second term).  $T_{m,c}$  and  $\rho_{m,c}$  are considered as the average values of the inlet and outlet of the collector. To consider the change of density due to temperature change, we consider the Boussinesq approximation as follows,

$$\rho_{c,i} - \rho_{c,o} = \frac{\rho_{c,i}(T_{c,o} - T_{c,i})}{T_{c,i}} \quad (1.14)$$

In the collector, air temperature rises due to the available radiation and therefore density decreases proportionally with respect to the temperature that can be calculated by (1.14). The nominal value of the temperature rise in Manzanares SCPPS was 20K. Note that  $q''$  is the available solar insolation to the air, means due to the ground radiative factors and also heat losses from the collector  $q''$  is less than the ideal irradiance. We present our performance study due to the collector efficiency to cover all these factors in the result and discussion section.

### 1.2.2 Tower

The air flow in the chimney is considered as an adiabatic frictionless flow. The conservation equations for the one-dimensional steady state flow in variable-area

tower are similar to collector except having the gravity term in momentum and energy equations.

By following the same trend to find  $dp$  we get

$$dp = \left[ -\rho g dz + \frac{\dot{m}^2 dA}{\rho A^3} + \rho u^2 \left( \frac{dp}{p} - \frac{dT}{T} \right) \right] \quad (1.15)$$

By applying the energy equation, substitution  $dT = (-gdz - udu)/c_p$  and  $dp = -\rho(udu + gdz)$ , we can rewrite the above equation as

$$dp = \left[ -\rho g dz + \frac{\dot{m}^2 dA}{\rho A^3} + \rho u^2 \left( \frac{dp}{p} - \frac{dp}{\rho c_p T} \right) \right] \quad (1.16)$$

Also by considering the material properties of air the same way we did for the collector part,

$$dp \simeq \left[ -\rho g dz + \frac{\dot{m}^2 dA}{\rho A^3} \right] \left[ 1 - \frac{2.494u^2}{T} \right]^{-1} \quad (1.17)$$

The above equation is the exact closed form solution for  $dp$  at any point as the function of variables  $\rho$ ,  $T$ . The last term on the RHS can be assumed to equal unity as we mentioned in the collector part. Let integrate between the inlet and outlet tower area to find the pressure difference of the chimney as,

$$\int_{t,i}^{t,o} dp \simeq \int_{t,i}^{t,o} \left( -\rho g dz + \frac{\dot{m}^2 dA}{\rho A^3} \right) \quad (1.18)$$

$$p_{t,o} - p_{t,i} \simeq -\rho_{m,t}gh_t - \frac{\dot{m}^2}{2\rho_{m,t}} \left( \frac{1}{A_{t,o}^2} - \frac{1}{A_{t,i}^2} \right) \quad (1.19)$$

Where  $\rho_{m,t} = (\rho_{t,i} + \rho_{t,o})/2$  and we can correlate the outlet tower pressure to the atmospheric density and the inlet collector pressure for an adiabatic tower,  $p_{c,i} = p_{t,o} + \rho_{\infty}gh_t$ . The air density change can be calculated by lapse rate temperature change due to the height change  $T_{t,o} = T_{\infty} - gh_t/c_p$ . Therefore by applying equation (1.14) in the polytropic EOS we obtain,

$$p_{t,o} = p_{\infty} \left( 1 - \frac{gh_t}{c_p T_{\infty}} \right)^{\left( \frac{c_p}{R} \right)} \quad (1.20)$$

We calculate the density at the tower outlet by having the tower outlet pressure from EOS. For an adiabatic tower-collector connection, if we do not consider a turbine (pressure change) in our model, we can assume  $\rho_{t,i} = \rho_{c,o}$ .

Also  $T_{\infty} = T_{c,i}$  and we can rewrite equation (1.14) as follows,

$$\rho_{t,i} = \rho_{c,o} = \rho_{\infty} \left( 1 + \frac{T_{\infty} - T_{c,o}}{T_{\infty}} \right) \quad (1.21)$$

In Manzanares prototype the circular cross sectional area of the tower does not change, therefore for the pressure difference at the tower we obtain,

$$p_{t,o} - p_{t,i} \simeq -\rho_{m,t}gh_t \quad (1.22)$$

### 1.2.3 Turbine

The Manzanares SCPPS turbine was mounted freely from the collector on a steel framework 9 m above ground level (see Fig 1.2). Four turbine blades are adjustable according to the face velocity of the air in order to achieve an optimal pressure drop across the turbine blades [1]. To calculate the output power, we can define the power on the basis of the pressure difference at the turbine – where it is normally utilized at the outlet of the collector and inlet of the tower. Change of the static pressure converts into rotational mechanical work. The ideal available power from the pressure difference is proportional to the mass flow rate and the pressure drop at the turbine location.



FIGURE 1.2: Manzanares prototype turbine [4].

$$\dot{W} \simeq \frac{\dot{m}(p_{c,o} - p_{t,i})}{\rho_{turb}} \quad (1.23)$$

For area the following equations is used, where  $b$  is an arbitrary positive real constant.

$$A_{c,i}^2 = bA_{c,o}^2, \quad (1.24)$$

Let  $\rho_{turb} = (\rho_{c,o} + \rho_{t,i})/2$  and substitute equations  $p_{c,o}$  and  $p_{t,i}$  from (1.13) and (1.22). Hence for the flow power by assuming  $p_{c,i} = p_{t,o} + \rho_{\infty}gh_t$ , we have

$$\dot{W} \simeq \frac{\dot{m}}{(\rho_{c,o} + \rho_{t,i})/2} \left[ \frac{-\dot{m}^2}{2\rho_{m,c}} \left( \frac{b-1}{bA_{c,o}^2} \right) + \frac{q'' \dot{m}}{2\pi h_c^2 c_p \rho_{m,c} T_{m,c}} \ln \frac{r_{c,i}}{r_{c,o}} + (\rho_{\infty} - \rho_{m,t})gh_t \right] \quad (1.25)$$

The first term on RHS of equation (1.25) presents the effect of the flow area change and it reduces the available pressure difference with respect to the typical shape of SCCPS. The second term represents the effect of the available solar radiation to the collector and the third term calculates the stack effect with respect to the available mean density difference along the tower and before the turbine. To calculate the output power from the available pressure difference in a realistic form, we consider,

$$P_t = \eta_c \dot{W} \quad (1.26)$$

Where  $\eta_c$  is the collector efficiency factor. Based on the 1982 experiments [1], the reported value, 0.32, for the Manzanares prototype collector efficiency would be considered in this analysis.

### **1.3 Numerical Analysis**

To perform CFD analysis, the finite volume method was employed via ANSYS/FLUENT M&S package. The air flow as an ideal gas under Boussinesq effect by solar irradiation was simulated. In the present CFD analysis the mass flow rate, obtained from the CFD results, along with other parameters were used to evaluate the maximum mechanical power for each case. The flow of air in SCPPS was assumed steady (in the average flow sense) and axisymmetric with respect to the chimney centerline. The meshed SCPPS axisymmetric model is shown in Fig. 1.3 with the details of applied boundary condition. ANSYS ICEM (Integrated Computer Engineering and Manufacturing) CFD was employed to generate a quadrilateral cell mesh. To perform the CFD simulation, the standard  $k - \epsilon$ , which is classified as a two-equation turbulence model, was applied. In this model, with respect to the sensitivity of the pressure solver to the density change, the density of air is calculated from the ideal gas equation. Stated differently, EOS was applied to calculate the air density with respect to the updated values of the pressure and temperature from the Navier Stokes equation results. The pressure boundary conditions at the entrance of the collector and the outlet of the chimney were assumed as atmospheric pressure and identical. The discretization accuracy of the

CFD solver is second order upwind for the density and momentum equation. Semi-implicit method for pressure-linked equations (SIMPLE) algorithm was applied as the pressure-velocity coupling to solve the pressure field. The chimney wall and the collector roof were considered adiabatic and the solar radiation was introduced to the ground as a constant heat flux. The residual criteria for all equations were set to be calculated and iterated not to exceed  $10^{-6}$ . The calculations were done by using a 16-core, 32 GB RAM computer.

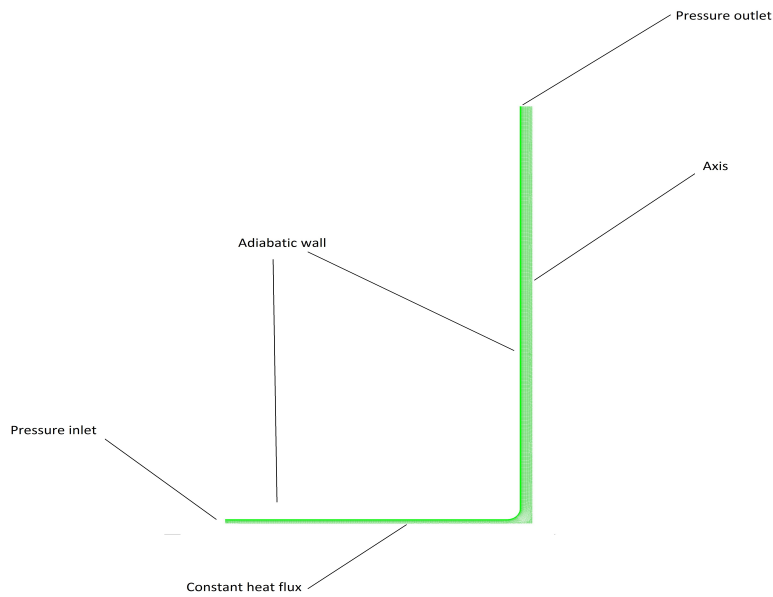


FIGURE 1.3: Computational domain and applied boundary conditions.

## 1.4 Results and Discussion

To evaluate the derived analytical solution for the output power of SCPPS, the available experimental data from Manzanares prototype was applied and extracted. The measured updraft velocity of Manzanares power plant for 24 hours operation

is substituted into the analytical solution (equation (1.26)) and compared against the experimental output power from the turbine (Fig. 1.4). Figure 1.4 presents the sixth order polynomial trend of data. Considering a constant collector efficiency ( $\eta_c$ ) as 0.32 for the whole 24-hour analysis, the total output power would be closer against the experimental data for higher solar radiation. The initial difference between the analytical and experimental values—light orange area (Fig. 1.4)—is due to the minimum stack effect (chimney effect) by considering the minimum reported measured velocity— 2 m/s during 12-1 am —flowing up to the chimney by the height of 194.6 m. However, it was obtained from the experimental analyses that the turbine has a minimum start up updraft velocity as 2.5 m/s and would not rotate for low velocities. Based on reported values from the Manzanares prototype [1] the maximum measured output power for 9m/s updraft velocity was 50kW—without any decimal precision. By imposing the same updraft velocity (9 m/s) at the turbine location, and applying the same collector efficiency (32%) and loss factor (0.9) the analytical output power would be 51.26 kW.

To have the characteristics of the Manzanares prototype we study the sensitivity of the analytical output power correlation to the mass flow rates. Therefore, the effect of mass flow rate on each terms of the total pressure change, including, inter alia, air flow geometry, solar radiation and stack effect would be observed. We performed this sensitivity analysis for a range of solar irradiation versus mass flow rate. It is observed that by increasing the mass flow rate the output power increases as long as the stack effect dominated the negative pressure difference due to the change of flow area. The dominant terms in the total pressure difference

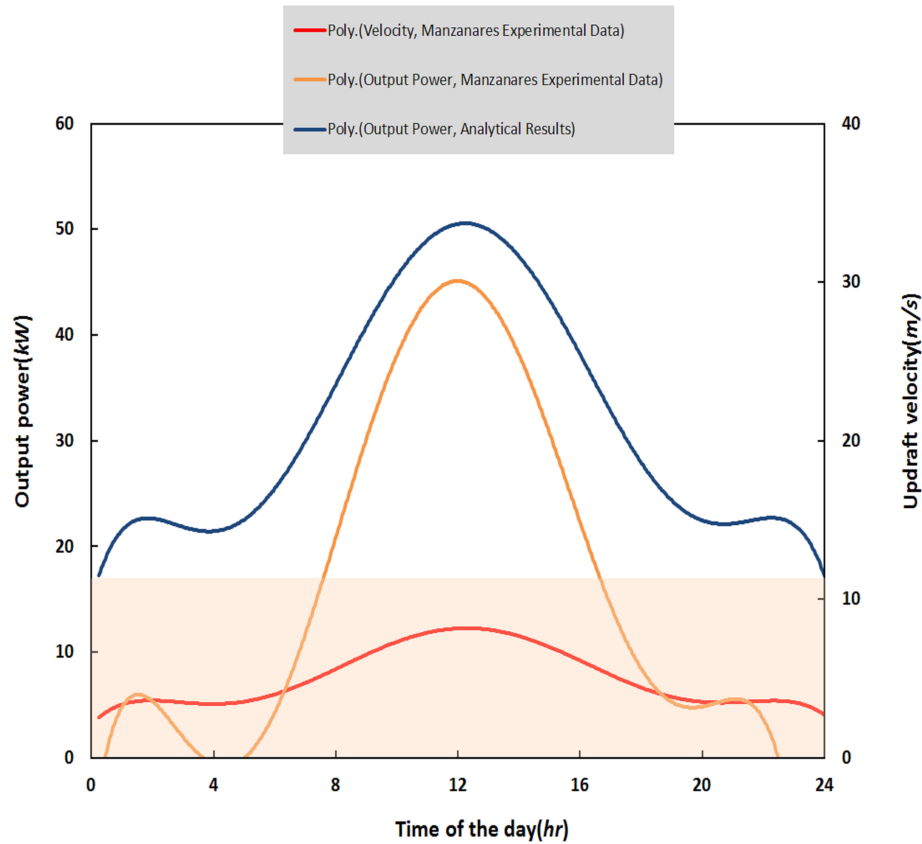


FIGURE 1.4: Analytical power results against measurement from Manzanares: updraft velocity and power output for a typical day.

are the flow area change and the stack effect terms. Since the flow is well within subsonic range, the inlet and outlet flow areas of the collector play the same role as nozzles and the pressure change of the nozzle flow is negative. By increasing the flow rate we reach to the theoretical maximum output power for each amount of solar irradiation. However, after the maximum power the dominant term is the negative pressure change due to the air flow area. Stated differently, after reaching to the the maximum theoretical output power, the positive-pressure change which rotates the turbine blade decreases by growing the pressure drop term due to the nozzle effect (Fig. 1.5). As it was mentioned before and shown in figure 1.5, the maximum power for the experimental velocity ( $9 \text{ m/s}$ ) is  $51.2 \text{ kW}$ . However, the maximum theoretical power from the characteristics of Manzanares SCPPS for

1000 ( $W/m^2$ ) solar irradiation is 51.8 kW. The output power characteristics with respect to mass flow rate can be useful for design or rating step of SCCPS.

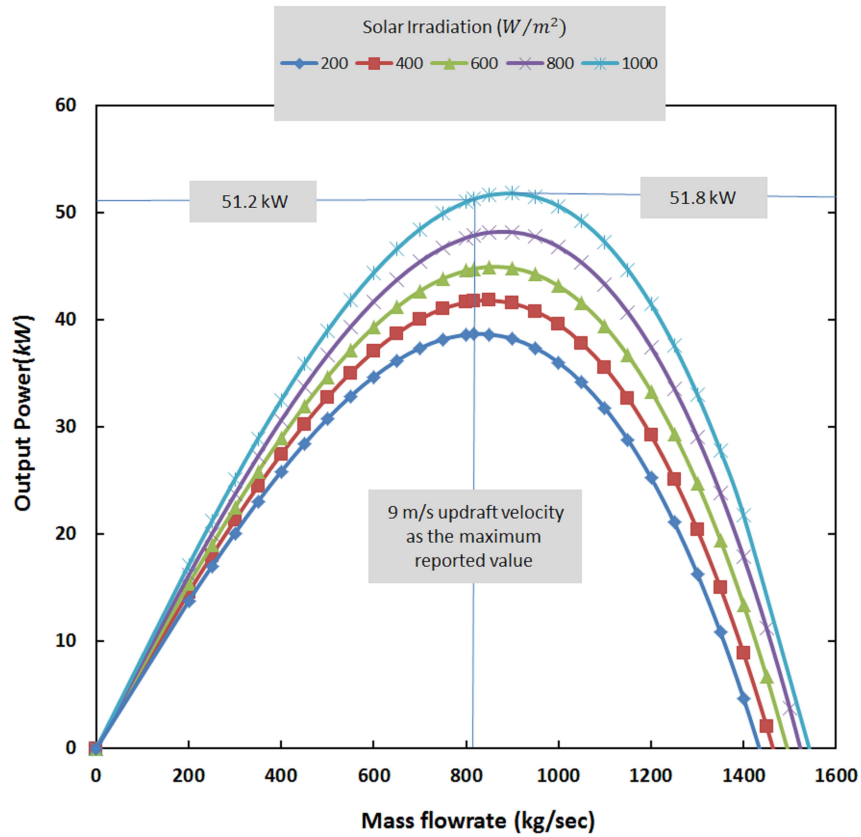


FIGURE 1.5: Analytical power results against mass flow rate for a range of solar irradiation.

To study the role of collector efficiency factor, we calculate the analytical output power for the maximum reported solar irradiation as the operating reported case for the output power of 50kW. Figure 1.6 depicts the logarithmic scale variation of output power with respect to a range of mass flow rate for different collector efficiency factors. Collector efficiency factor varies from 0.1 to 1 and can be considered as the overall adjusted efficiency factor. The ideal ( $\eta_c = 1$ ) maximum output power for 1000 ( $W/m^2$ ) solar irradiation is 161.7 kW from the analytical solution (Fig 1.6).

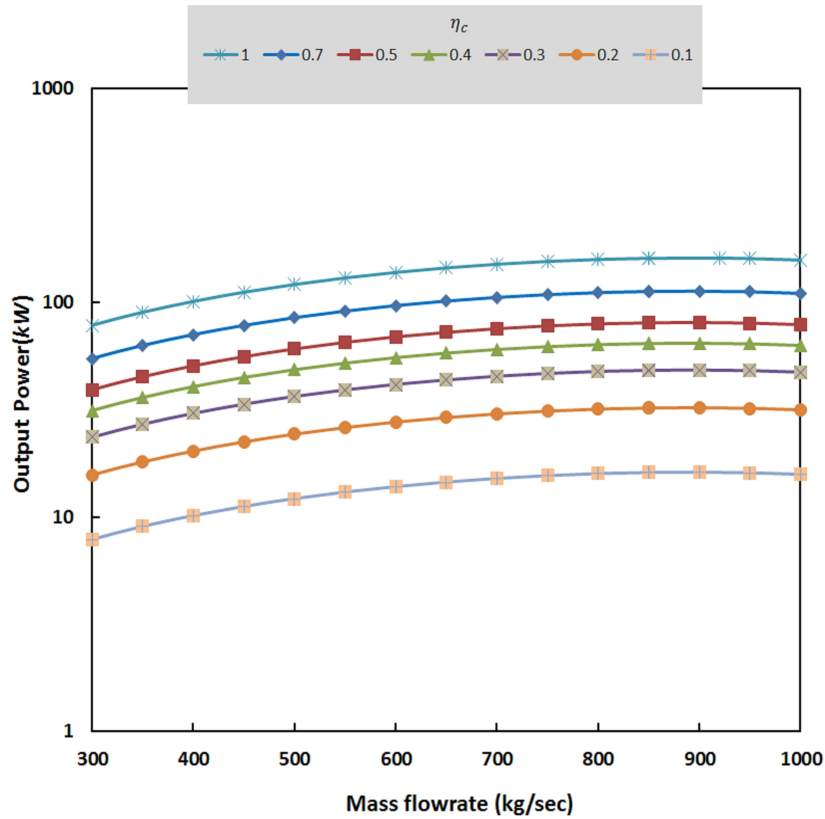


FIGURE 1.6: Analytical power results against mass flow rate for different values of collector efficiency.

To obtain the available power to rotate the turbine, the kinetic energy of the air flow at the outlet of the collector was calculated. For each CFD analysis (Fig. 1.7), the mass flow rate and the average density at the turbine location are gained from the numerical simulation result and used to calculate the available kinetic energy per time. The calculated available power for different solar irradiation are compared against the experimental data and the analytical solution in two cases. Analytic-EXP shows the power where the average velocity were obtained from the available experimental data at the same amount of reported radiation. It is needless to say that details of available experimental data are not clear enough to report the data with all sources of uncertainty(Fig. 1.8). The reliability of experimental data is suggested to measure for future works. CFD results were

performed under the ideal assumption of having no heat loss from the tower or collector. Also we imposed the available heat flux as a boundary condition. Stated differently, in the CFD analysis we introduced the flow domain e.g.  $1000 \text{ W/m}^2$  where in the experiment the amount of reported velocity at  $1000 \text{ W/m}^2$  solar radiation is lower because of the absorptivity factor of the collector ground. The available power at the turbine location, CFD in Fig. 1.7, by using the CFD values for density and velocity were calculated based on the rate of kinetic energy,  $0.5\dot{m}u^2$ . Two different ratios of the available kinetic energy at the turbine location are used for SCCPS analysis. One is referred as Betz criterion or Betz limit which is  $16/23$  and was formulated in 1919. Betz criterion is the theoretical power fraction that can be extracted from an ideal wind stream. The other one is  $2/3$  and were used in several investigations. The CFD results that have been calculated by Betz criterion and  $2/3$  are shown as CFD-Betz and CFD- $2/3$  respectively (Fig. 1.8). It is shown as CFD-Betz The difference between the available power from simulation results (CFD) and the experimental turbine power is due foremost to the turbine efficiency and then having no heat loss in the CFD model.

## **1.5 Conclusion**

We presented a combined numerical-analytical analysis for solar chimney power plant, based on the Manzanares prototype. The harvestable power of Manzanares power plant was investigated as the function of available solar irradiation and mass flow rate. The CFD M&S was carried out. Also the one-dimensional analytical analysis was done with attention to underlying assumptions and simplifications.

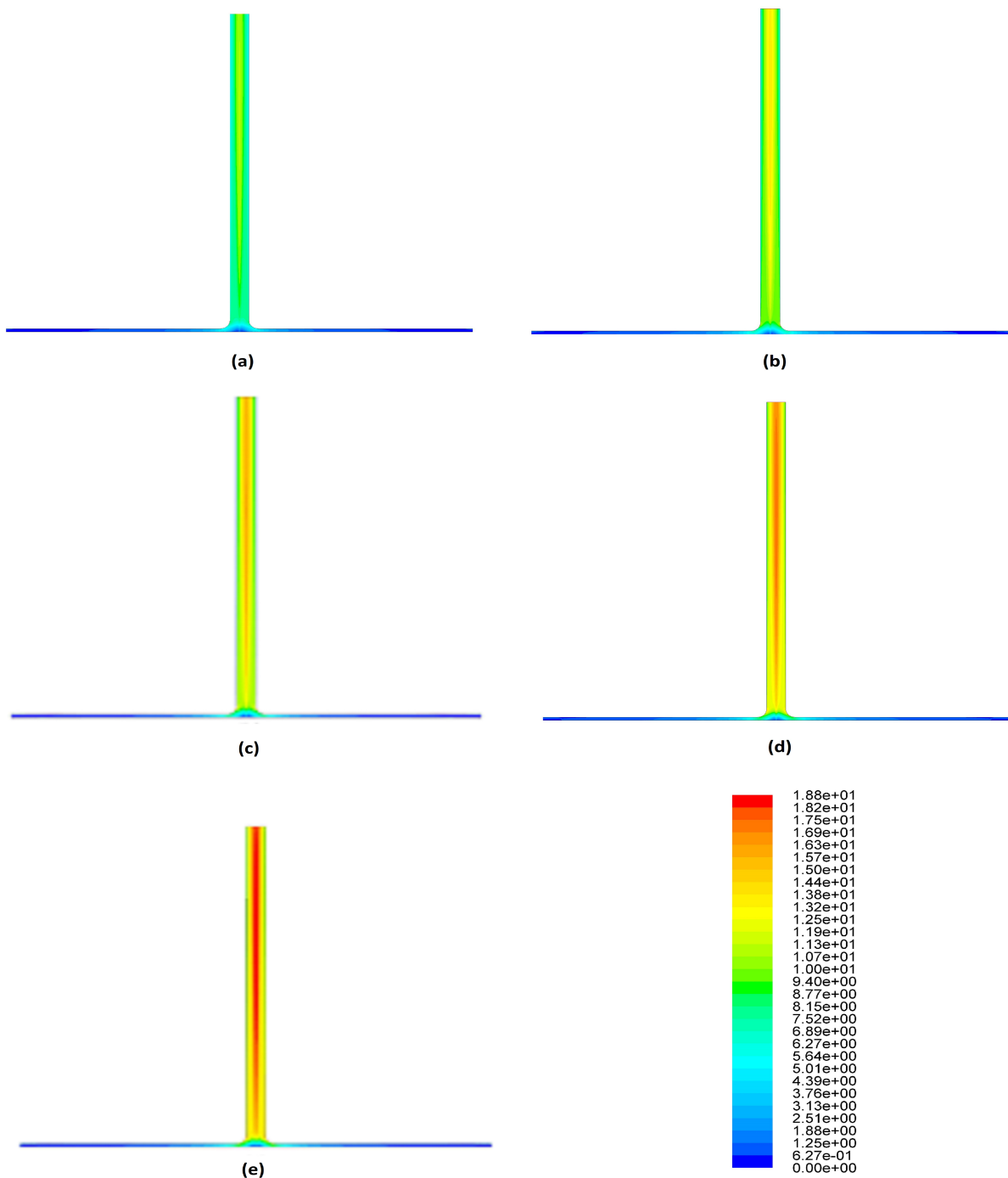


FIGURE 1.7: Velocity contour plot ( $m/s$ ) for different available solar heat flux at the ground of collector, (a):200, (b):400, (c):600, (d):800, (e)1000  $W/m^2$ .

We compared the numerical results against the available limited raw experimental data from the prototype and also showed the range of reliability of the analytical solution. Where the inlet velocity values for analytical correlation were obtained

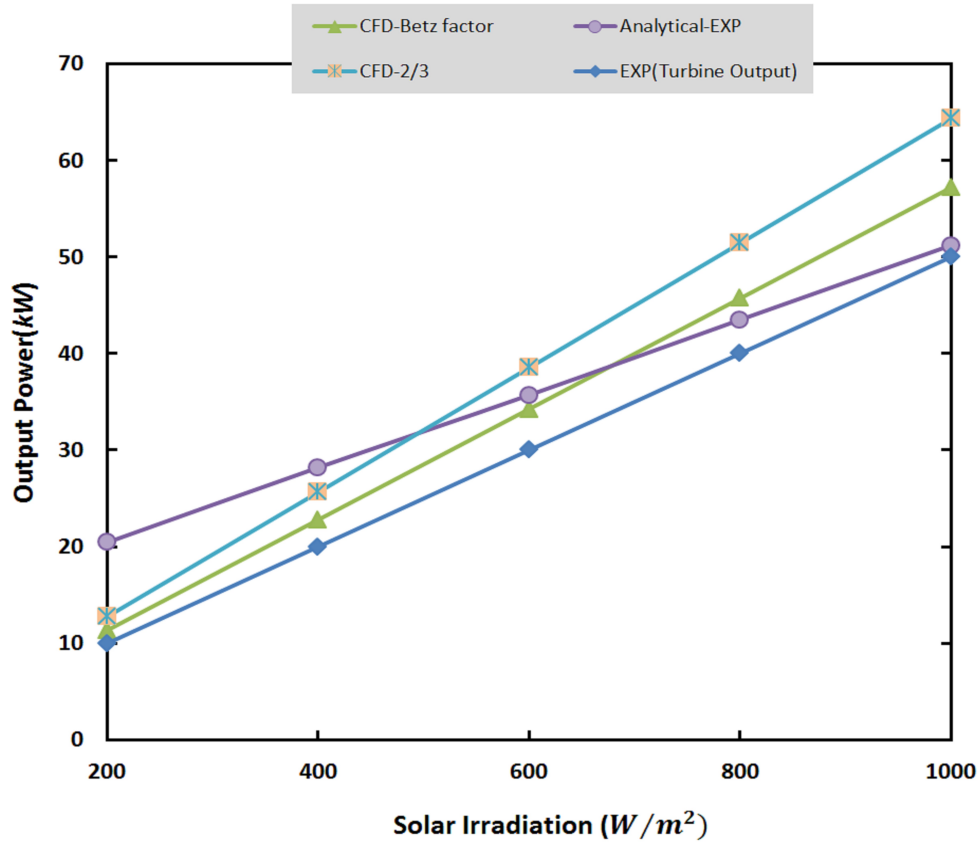


FIGURE 1.8: Power vs solar irradiation.

from the experimental velocities we got higher available power than the output turbine power. This difference increases for lower solar irradiation and mass flow rate values due to the stack effect term in the analytical solution. That has several reasons as, (a) The one dimensional analytical solution has several simplifications, including treatment of average density and the heat flux term., (b) It is very important to pick the right source to impose the values to the analytical correlation., (c) Available experimental data are not just limited, but also not extensively characterized in terms of uncertainty and repeatability, making it difficult to produce error bars on experimental values for a prescribed level of confidence. To present the volatility of the analytical correlation, we selected two

different approaches to input values in this one-dimensional equation; I- Imposing the experimental velocities and calculation densities with respect to average temperature., II- Applying a range of mass flow rates to obtain the characteristics of Manzanares prototype analytically. During the verification and validation process, the modeler must ask two questions: *Am I modeling the physics correctly?* and *Am I modeling the correct physics?* Comparison with analytical models is important for answering both of these questions, and the only way to have them well-posed is to have correct physics in the analytics.

# Bibliography

## References

- [1] Haaf, W., K. Friedrich, G. Mayr, and J. Schlaich. "Solar chimneys part I: principle and construction of the pilot plant in Manzanares." *International Journal of Solar Energy* 2, no. 1 (1983): 3-20.
- [2] Haaf, W. "Solar chimneys: part ii: preliminary test results from the Manzanares pilot plant." *International Journal of Sustainable Energy* 2, no. 2 (1984): 141-161.
- [3] Schlaich, Jörg, Michael Robinson, and Frederick W. Schubert. *The solar chimney: electricity from the sun*. Geislingen, Germany: Axel Menges, (1995).
- [4] Schlaich, Jorg, Rudolf Bergermann, Wolfgang Schiel, and Gerhard Weinrebe. "Design of commercial solar updraft tower systems—utilization of solar induced convective flows for power generation." *Journal of Solar Energy Engineering* 127, no. 1 (2005): 117-124.
- [5] Zohuri, Bahman, and Nima Fathi. "Thermal-hydraulic analysis of nuclear reactors." New York: Springer, 2015.

- [6] Padki, M. M., and S. A. Sherif. "Solar chimney for medium-to-large scale power generation." In Proceedings of the manila international symposium on the development and management of energy resources, vol. 1, pp. 432-437. 1989.
- [7] Yan, M. Q., S. A. Sherif, G. T. Kridli, S. S. Lee, and M. M. Padki. "Thermo-fluid analysis of solar chimneys." In Industrial Applications of Fluid Mechanics-1991. Proceedings of the 112th ASME winter annual meeting, Atlanta, GA, pp. 125-130. 1991.
- [8] Von Backström, Theodor W., and Thomas P. Fluri. "Maximum fluid power condition in solar chimney power plants—an analytical approach." *Solar Energy* 80, no. 11 (2006): 1417-1423.
- [9] Putkaradze, Vakhtang, Peter Vorobieff, Andrea Mammoli, and Nima Fathi. "Inflatable free-standing flexible solar towers." *Solar Energy* 98 (2013): 85-98.
- [10] Fluri, T. P., and T. W. Von Backström. "Performance analysis of the power conversion unit of a solar chimney power plant." *Solar Energy* 82, no. 11 (2008): 999-1008.
- [11] Peter Vorobieff, Andrea Mammoli, Nima Fathi, and Vakhtang Putkaradze. "Free-standing inflatable solar chimney: experiment and theory." *Bulletin of the American Physical Society* 59 (2014).
- [12] Nima Fathi, Peter Vorobief, Seyed Sobhan Aleyasin. "V&V Exercise for a Solar Tower Power Plant." *ASME Verification and Validation Symposium* (2014).

<https://cstools.asme.org/csconnect/FileUpload.cfm?View=yes&ID=44167>

- [13] Zhou, Xinping, Jiakuan Yang, Bo Xiao, Guoxiang Hou, and Fang Xing. "Analysis of chimney height for solar chimney power plant." *Applied Thermal Engineering* 29, no. 1 (2009): 178-185.
- [14] Koonsrisuk, Atit, and Tawit Chitsomboon. "Theoretical turbine power yield in solar chimney power plants." In *Thermal Issues in Emerging Technologies Theory and Applications (ThETA)*, 2010 3rd International Conference on, pp. 339-346. IEEE, 2010.
- [15] Xu, Guoliang, Tingzhen Ming, Yuan Pan, Fanlong Meng, and Cheng Zhou. "Numerical analysis on the performance of solar chimney power plant system." *Energy Conversion and Management* 52, no. 2 (2011): 876-883.
- [16] Koonsrisuk, Atit, and Tawit Chitsomboon. "Mathematical modeling of solar chimney power plants." *Energy* 51 (2013): 314-322.
- [17] Zhou, Xinping, Fang Wang, and Reccab M. Ochieng. "A review of solar chimney power technology." *Renewable and Sustainable Energy Reviews* 14, no. 8 (2010): 2315-2338.
- [18] Koonsrisuk, Atit, and Tawit Chitsomboon. "Effects of flow area changes on the potential of solar chimney power plants." *Energy* 51 (2013): 400-406.